11th Int. Beam Instrum. Conf. IBIC2022, Kraków, Poland JACoW Publishing
ISBN: 978-3-95450-241-7 ISSN: 2673-5350 doi:10.18429/JACoW-IBIC2022-WEP25

INSTALLATION AND COMMISSIONING OF THE PULSED OPTICAL TIMING SYSTEM EXTENSION

F. Rossi*, M. Ferianis, Elettra Sincrotrone Trieste S.C.p.A., Trieste, Italy

Abstract

At the FERMI FEL user facility, a fully optical timing system has been operated, to synchronize it, since the start of machine commissioning, back in 2009. In the past years the system has been progressively extended to support more clients. The latest upgrade is focusing on the pulsed subsystem which provides the phase reference to remote lasers and the bunch arrival monitor diagnostic stations. In origin the pulsed subsystem had a capacity to feed simultaneously six stabilized fiber links. The upgrade to the original layout makes it possible to install up to eight new additional links. Here we will describe the new setup and the results achieved in terms of short- and long-term stability.

INTRODUCTION

FERMI [1] is a fourth generation light source, a seeded Free Electron Laser (FEL), operating as a user facility in Trieste, Italy. A state-of-art all optical timing and synchronization system [2] has been deployed implementing a hybrid architecture as a combination of pulsed and continuous wave techniques.

The pulsed optical timing subsystem generates and delivers with 10 femtosecond precision the reference to all phase critical FERMI clients, like lasers and longitudinal diagnostics. The installation started with two links in 2009 and, since then, has been progressively updated to the current configuration serving a total of six clients.

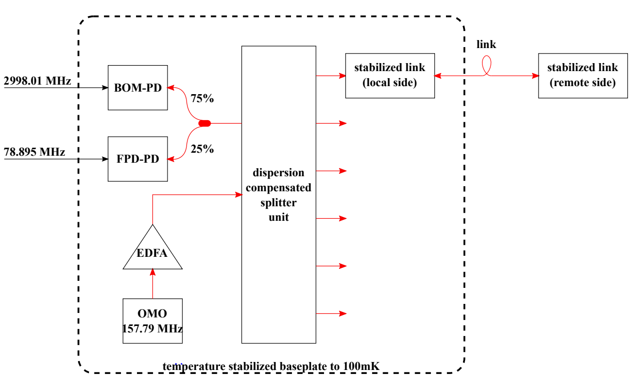

Figure 1: Block diagram of the original pulsed timing subsystem.

The block diagram of the subsystem originally installed is shown in Fig. 1. The optical master oscillator (OMO) is a soliton fiber laser working with a repetition rate of 157.79 MHz, i.e. one nineteenth of the 2998.01 MHz microwave frequency of the reference master oscillator (RMO). The OMO is phase locked to the RMO signal by a Balanced Optical Microwave Phase Detector (BOM-PD), while the ambiguity of the zero crossing selection is solved by using a Fast Photodiode Phase Detector (FPD-PD). The signal from the OMO, amplified by a single Erbium Doped Fiber Amplifier (EDFA), is delivered at the output ports of a splitter along a dispersion-compensated path. This one is entirely implemented in fiber and guarantees short pulses at the input of a stabilized link which is built around a balanced cross-correlator (BOCC). Six ports are dedicated to timing distribution purposes, other two are used to seed the phase detectors and, finally, one is reserved for the extension. Each splitter output port dedicated to the timing distribution provides pulses at 40 mW average power, while the full width at half maximum (FWHM) is about (165 ± 9) fs.

A progressive extension of the pulsed optical timing subsystem is expected in the coming years to feed new clients with the phase reference. To fulfil the installation requests of additional timing clients in FERMI (e.g. new bunch arrival monitor stations or a user laser oscillator) we have started working towards an upgrade of the original subsystem.

THE SLAVE SUBSYSTEM

The extension of the pulsed subsystem has been implemented by Cycle GmbH [3]. The design follows the same architecture of the original subsystem so the optical signal coming from a second port of the OMO is again amplified and split. The upgrade makes it possible to add up to eight new stabilized pulsed links to the timing system. The optical signal is mainly routed in fiber; along the path there is a minimal free-space section described below. One of the design requirements was to maintain mechanical and optical compatibility with the link stabilization units installed in the past.

The overall block diagram of the extended pulsed system is shown in Fig. 2. The part described in the previous section is called “master” while the new devices are hereafter indicated as “slave”. In fact the slave is locked to the master to remove residual timing drifts among the two splitters output ports. The key element of the tracking loop is a phase detector implemented by means of a BOCC. The error signal is used to drive an actuator – a combination of a fiber piezo stretcher and a motorized translation stage – to keep the pulses coming out from the outputs of the master and slave splitters synchronized. Part of the actuator block is also a manual free-space delay line used to align in time the pulses and set the zero-crossing of the BOCC in the dynamic range of the control loop.

There are two fiber interconnections between the master and slave subsystems at ports A and B. The former is included in the controlled path of the tracking system while

* fabio.rossi@elettra.eu

11th Int. Beam Instrum. Conf. IBIC2022, Kraków, Poland JACoW Publishing
ISBN: 978-3-95450-241-7 ISSN: 2673-5350 doi:10.18429/JACoW-IBIC2022-WEP25

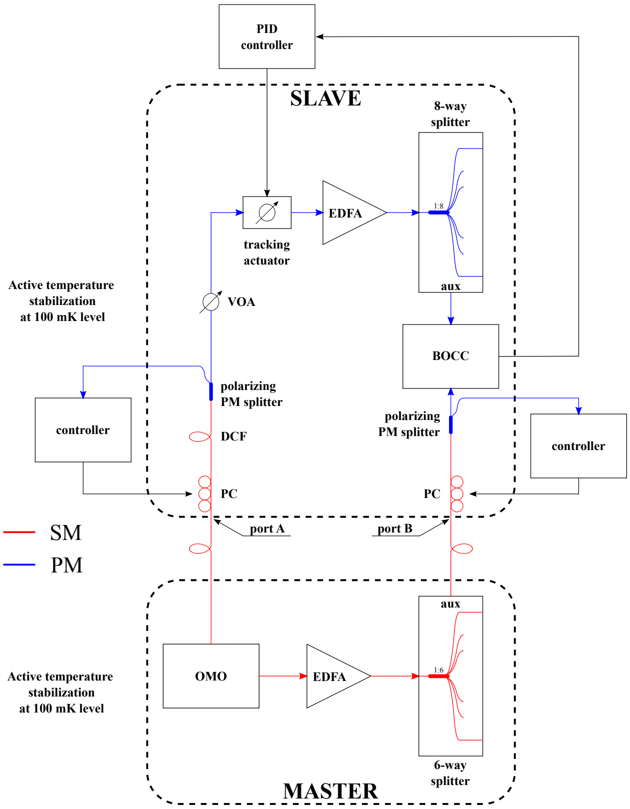

Figure 2: Simplified block diagram of the extended pulsed timing system. DCF: Dispersion Compensating Fiber, PC: Polarization Controller, PID: Proportional Integral Derivative, PM: Polarization Maintaining fiber, SM: Single Mode fiber, VOA: Variable Optical Attenuator.

the latter is the most critical from the point of view of the timing application. The fiber path at port B up to the BOCC must be as short as possible and temperature stabilized to avoid transferral of unwanted out-of-loop drifts that cannot be compensated.

The two subsystems mainly differ for the fiber type used which is polarization maintaining for the slave. For this reason, at the interface ports A and B there is a polarization controller used to set the proper state (linear along the slow axis) at the input of a polarizing fiber splitter. During the commissioning of the extension we have used the PCs in open loop mode though it is possible to control them for compensating polarization drifts of the signals arriving from the master subsystem. By using a PM design, the slave subsystem allows additional flexibility with regard to the choice of the new links. In case of more demanding requirements they might even be built with polarization maintaining technology.

The master and slave subsystems are sitting on the same optical table, in independent enclosures, each one using its own water-cooled baseplate. Moreover the aluminium baseplate of the slave is thermally insulated on the bottom face. The cooling systems of the two baseplates are also independent to avoid galvanic corrosion since they are made of different materials. The slave enclosure uses damping feet accurately chosen to attenuate mechanical vibrations. The side panels and the top lid integrate sheets of foam for the same purpose.

CHARACTERIZATION

During the commissioning of the extension we evaluated many aspects of the slave subsystem. Only the most relevant results will be reported here. A few characterizations have been done on a long-term timescale, described in the next section, in which cases the acquisition period lasted for a minimum of 24 hours.

Optical Signal Integrity

The shape of the optical pulses after the splitter has a direct impact on the fiber link stabilization units and in particular the behaviour of the femtosecond timing detector. The cross-correlation signal must show a unique zero-crossing point centered along a strictly monotonic transition - better with a constant slope - between maximum and minimum points. The design of the amplifier and the dispersion compensated path in the slave subsystem should therefore guarantee the integrity of the pulses. In order to achieve minimized distortion of their temporal profile, the autocorrelation taken at the splitter port should have a single central lobe and avoid as much as possible the presence of satellites.

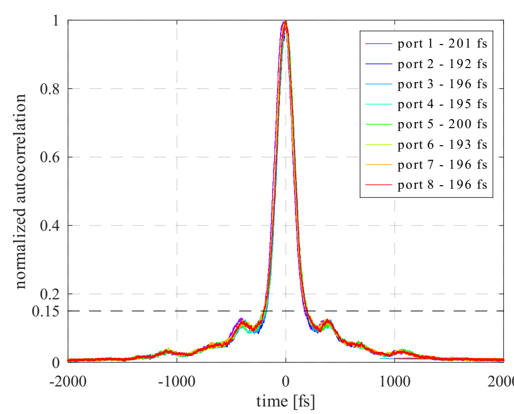

Figure 3: Autocorrelations after the slave splitter.

The working point of the slave subsystem must be accurately chosen by tuning the input power to the EDFA, by means of a VOA, and the gain value of the amplifier itself in order to match the specifications in terms of output pulse integrity, power and duration. The propagation along the fiber of the optical pulses from the OMO is affected by dispersion and non-linear effects due to the high power level between the amplifier output and the splitter. The average power available at each of the splitter output ports is more than 45 mW.

The dispersion compensated path has been designed to have a FWHM pulse duration less than 200 fs assuming a Gaussian shape. In Fig. 3 the measurements acquired with a FemtoChrome FR-103XL instrument are presented; the

ISBN: 978-3-95450-241-7 ISSN: 2673-5350 doi:10.18429/JACoW-IBIC2022-WEP25

result is (196 ± 5) fs FWHM. The autocorrelation of all the slave subsystem outputs shows a pedestal whose relative height has been optimized to be lower than 15% of the main central lobe.

The pedestal is due to residual uncompensated non-linear effects accumulated during the propagation in the fiber. Even if the autocorrelation is not optimal, we have verified that this result does not entail major issues with the downstream cross-correlations (e.g. for the link stabilization or remote client synchronization). In Fig. 4 we report examples of BOCC outputs used in the system characterization. In particular, the typical error signal used to lock the slave subsystem to the master is shown in Fig. 4a. A distortion is visible related to the signal integrity of the pulses but we consider it as a second order problem because the tracking loop works around the zero-crossing.

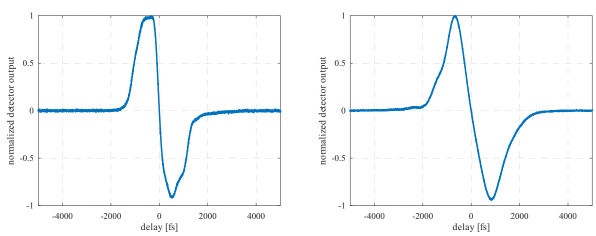

(a) (b)

Figure 4: Typical normalized cross-correlations: a) between the master and slave splitter outputs; b) between the OMO and one output of the slave splitter.

Relative Intensity Noise (RIN)

The optical signal at the output from the splitter is attenuated to operate the detection photodiode (battery powered EOTech ET-3500F) in the linear regime. Before entering a low noise baseband amplifier the electrical output from the detector is low-pass filtered. The voltage spectral density is then acquired by using the baseband input channel of a Keysight E5052B signal source analyzer (SSA). The relative intensity noise is calculated after a normalization of the acquired signal to the measured DC output from the amplifier.

The RIN performance depends on the EDFA working point; the best result we achieved is shown in Fig. 5. The orange trace (right axes) represents the partial integration from the given offset frequency to the amplifier bandwidth. The integrated RIN in the 10 Hz – 5 MHz bandwidth is 0.052% RMS compared to the 0.037% RMS value for the OMO measured with the same setup. The tracking loop status doesn't affect the result.

Additive Timing Jitter

The short-term stability achievable by the slave subsystem mostly depends on the EDFA in the chain between the OMO and the splitter output ports. For the characterization of this contribution we have measured the cross-correlation between the laser (it has a third output port not visible in Fig. 2)

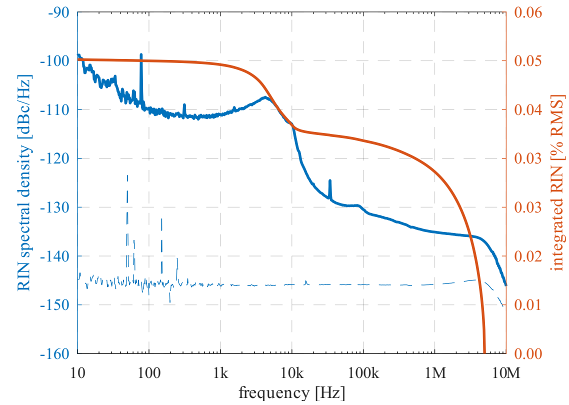

Figure 5: RIN measured after the slave splitter. The blue dashed trace represents the noise floor of the measurement setup. It is visible the cut-off frequency of the amplifier.

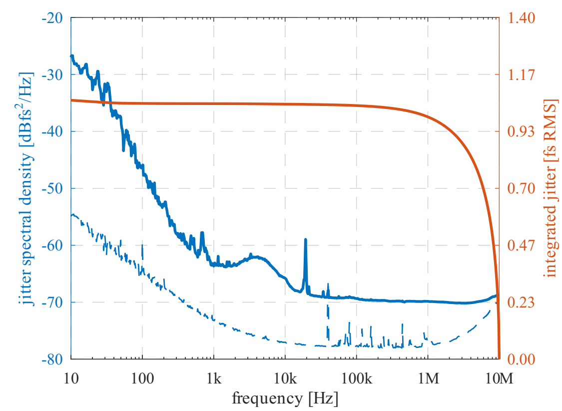

Figure 6: Additive jitter of the slave subsystem. The blue dashed trace represents the noise floor of the measurement setup.

and one of the ports of the slave splitter. The normalized signal used for the calibration is visible in Fig. 4b.

The jitter spectral density of the BOCC output in the zero-crossing acquired by the SSA is shown in Fig 6. The photodetector in the BOCC is the Thorlabs PDB450A with 1×10^4 transimpedance gain. In that configuration the detector supports the full analysis bandwidth 10 Hz – 10 MHz of the instrument, the integrated jitter is 1.1 fs RMS.

LONG-TERM MEASUREMENTS

Splitter Stability

The length mismatch of the splitter output pigtails was accurately evaluated by means of an external BOCC unit. We have compared a reference signal on one side and, sequentially, all the output ports of the splitter on the other side. The length difference was obtained by measuring the zero-crossing temporal shift of the cross-correlator output. The maximum difference measured among all the splitter ports is 1.16 mm. This result guarantees the interchangeability of the

ISBN: 978-3-95450-241-7 ISSN: 2673-5350 doi:10.18429/JACoW-IBIC2022-WEP25

splitter ports with a minimum acceptable phase difference if the relocation of a link stabilization unit is needed.

Even if the length equalization among the output ports described above is very good, a temperature control of the splitter box is mandatory to avoid residual drifts that cannot be compensated afterwards by the link stabilization units. The active temperature control allows to achieve a stabilization better than 10 mK over many days of operation.

The timing stability between two splitter ports was measured with an external BOCC unit installed in the slave enclosure. The result is shown in Fig. 7. The drift visible at the beginning relates to the initial transient (first three hours) needed for the stabilization of the setup. The peak to peak variation after the transitory is less than 6 fs over a 24-hour interval. We think it doesn't show the real performance but only a limit of the measurement setup itself.

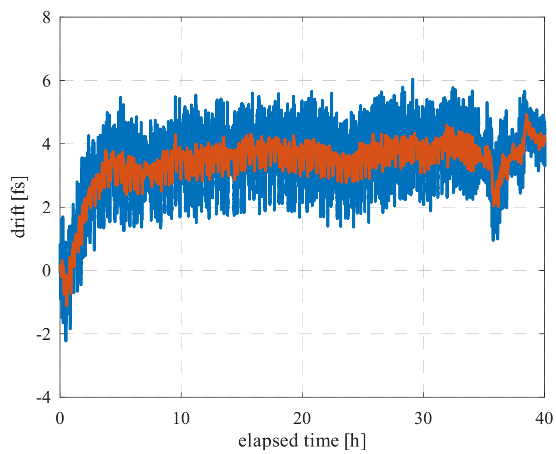

Figure 7: Long-term stability between two slave splitter ports.

Tracker Performance

The final and most demanding test was the characterization of the residual drift between the master and slave splitters with the tracker loop in operation. This measurement is quite challenging because the two subsystems are physically independent. Although they are on the same optical table each one is installed in its own enclosure. The typical result is shown in Fig. 8 where the residual drift is less than 20 fs peak to peak over a 24-hour interval.

The drift has been measured with an out-of-loop balanced cross-correlator installed inside the slave enclosure. The interconnection between the master and the BOCC adds an uncompensable drift to the result and limits the minimum value achievable with this setup. In our case it was implemented with a 2 m SMF fiber patch cord installed mostly inside the two splitter units which are temperature controlled with a peak to peak stability better than 10 mK. If we assume that the thermal coefficient of delay is typically in the order of a few tens of fs/m/K then the impact of the out-of-loop fiber on this measurement can be estimated in the order of a few femtoseconds.

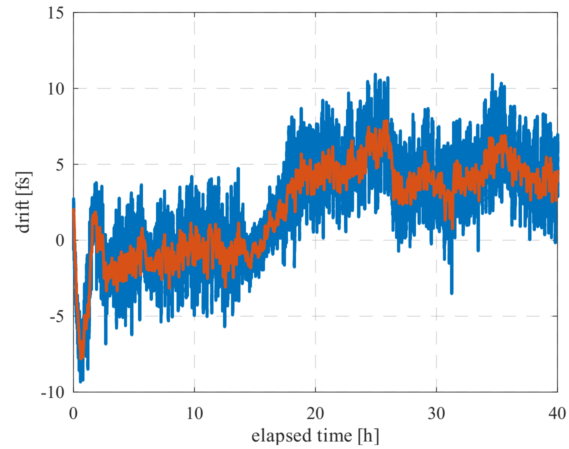

Figure 8: Long-term stability between master and slave subsystems with tracker loop active.

Even if the fibers of the master subsystem are temperature controlled, the polarization at ports A and B is slightly drifting, this has an impact on the behaviour of the tracking system and is probably limiting the long-term performance reported in this section.

CONCLUSIONS AND FUTURE WORK

We have validated the design and implementation of the pulsed timing subsystem extension. Before putting it in operation on a daily basis we will carry out monitoring for a longer period to evaluate its reliability. Furthermore an integration of the new hardware in the machine control system is mandatory.

In the future we will investigate about the issues regarding the polarization stability between the master and slave subsystems. We are also planning to install a testing stabilized short link in the laboratory between the two splitters or, alternatively, compare at the remote location the relative stability of two links connected to the master and slave subsystems, respectively.

ACKNOWLEDGEMENTS

The authors would like to thank Anan Dai, Marvin Edelmann, Franz Kaertner and Kemal Shafak from Cycle GmbH for the discussions and support during the in-house system commissioning.

REFERENCES

[1] E. Allaria *et al.*, "Highly coherent and stable pulses from the FERMI seeded free-electron laser in the extreme ultraviolet", *Nat. Photonics*, vol. 6, no. 9, 2012. doi:10.1038/nphoton.2012.233

[2] M. Ferianis, A. O. Borga, A. Bucconi, M. Predonzani, F. Rossi, and L. Pavlovic, "All-optical Femtosecond Timing System for the Fermi@Elettra FEL", in *Proc. FEL'11*, Shanghai, China, Aug. 2011, paper FROAI2, pp. 641–647.

[3] https://www.cyclelasers.com